Abstract

Title:	ASSESSING THE INFLUENCE OF ABIOTIC FACTORS AND LEAF-LEVEL PROPERTIES ON THE STABILITY OF GROWING-SEASON CANOPY GREENNESS IN A DECIDUOUS FOREST
	Vanessa Marie L. Cunningham,
	Masters of Science, 2016
Thesis directed by:	Professor David Nelson
	UMCES Appalachian Laboratory
	Professor Andrew Elmore
	UMCES Appalachian Laboratory

Maps depicting spatial pattern in the stability of summer greenness could advance understanding of how forest ecosystems will respond to global changes such as a longer growing season. Declining summer greenness, or "greendown", is spectrally related to declining near-infrared reflectance and is observed in most remote sensing time series to begin shortly after peak greenness at the end of spring and extend until the beginning of leaf coloration in autumn,. Understanding spatial patterns in the strength of greendown has recently become possible with the advancement of Landsat phenology products, which show that greendown patterns vary at scales appropriate for linking these patterns to proposed environmental forcing factors. This study tested two non-mutually exclusive hypotheses for how leaf measurements and environmental factors correlate with

greendown and decreasing NIR reflectance across sites. At the landscape scale, we used linear regression to test the effects of maximum greenness, elevation, slope, aspect, solar irradiance and canopy rugosity on greendown. Secondly, we used leaf chemical traits and reflectance observations to test the effect of nitrogen availability and intrinsic water use efficiency on leaf-level greendown, and landscape-level greendown measured from Landsat. The study was conducted using *Quercus alba* canopies across 21 sites of an eastern deciduous forest in North America between June and August 2014. Our linear model explained greendown variance with an R^2=0.47 with maximum greenness as the greatest model effect. Subsequent models excluding one model effect revealed elevation and aspect were the two topographic factors that explained the greatest amount of greendown variance. Regression results also demonstrated important interactions between all three variables, with the greatest interaction showing that aspect had greater influence on greendown at sites with steeper slopes. Leaf-level reflectance was correlated with foliar $\delta^{13}C$ (proxy for intrinsic water use efficiency), but foliar $\delta^{13}C$ did not translate into correlations with landscape-level variation in greendown from Landsat. Therefore, we conclude that Landsat greendown is primarily indicative of landscape position, with a small effect of canopy structure, and no measureable effect of leaf reflectance. With this understanding of Landsat greendown we can better explain the effects of landscape factors on vegetation reflectance and perhaps on phenology, which would be very useful for studying phenology in the context of global climate change

ASSESSING THE INFLUENCE OF ABIOTIC FACTORS AND LEAF-LEVEL PROPERTIES ON THE STABILITY OF GROWING-SEASON CANOPY GREENNESS IN A DECIDUOUS FOREST

By

Vanessa Marie L. Cunningham

Thesis submitted to the Faculty of the Graduate School of the University of Maryland, College Park in partial fulfillment of the requirements for the degree of
Masters of Science
2016

Advisor Committee:

Professor David Nelson, Chair

Professor Andrew Elmore

Professor Brenden McNeil

Contents

Introduction

A shift in vegetation phenology has been one of the most measurable impacts of climate change on forested ecosystems (Bonan, 2008; Cleland et al., 2007; Menzel and Fabian, 1999jackson; Saxe et al., 2001). In temperate forest of the Northern Hemisphere, leaf development has been advancing in spring, whereas leaf senescence in autumn has been occurring later, effectively lengthening the duration of the growing season (Jeong et al., 2011; Menzel and Fabian, 1999; Zhou et al., 2001). A longer growing season potentially has a significant impact on the carbon, energy, and water cycles (Bonan, 2008; Fitzjarrald et al., 2001; Keeling et al., 1996; Richardson et al., 2006). Spatially, broad-scale phenology patterns are defined well by climatic and environmental gradients; i.e., for every 30-m increase in elevation spring is delayed ~1 day because of a change in environmental lapse rates (Hopkins, 1918). However, there is considerable fine-scale spatial variability in phenology that is driven by local factors, such as topography, species composition, and disturbance history (Cook et al., 2012; Elmore et al., 2012; Fisher et al., 2006; Morisette et al., 2009; Richardson et al., 2006; Zhang et al., 2004a). An example of such local effects is the urban heat-island effect (Zhang et al., 2004b). Therefore, disentangling the relative importance of potential controls on forest phenology requires data measured at scales relevant to the environmental variables driving spatial patterns.

Remote sensing of phenology recently increased in spatial resolution from $\geq$ 250m to 30m resolution with the advent of free Landsat data and the development of techniques to compile these data into dense stacks of surface reflectance (Masek et al., 2006). When vegetation measurements compiled from 30 years of Landsat data are

1

organized by day of year (DOY) and discarding year of acquisition, an average

phenology curve emerges that exhibits rich spatial variation in the trajectory of spring,

summer, and autumn canopy greenness (Elmore et al., 2012; Fisher et al., 2006; Melaas

et al., 2013). A spatially-variable, yet prevalent, pattern revealed in these data in eastern

deciduous forests is a gradual decline in summer greenness (hereafter called greendown),

consistently observed between peak greenness in early summer and the beginning of leaf

coloration in autumn (Elmore et al., 2012) (Figure 1). This decline in greenness is driven

by a decline in NIR reflectance, which influences remote sensing measures of greenness

(e.g., vegetation indices and vegetation fraction from spectral mixture analysis). Although

greendown is observed in studies of Landsat phenology (Elmore et al., 2012; Fisher et al.,

2006; Melaas et al., 2013), little information exists concerning how greendown varies

across landscapes in response to topography and canopy structure or how it might relate

to growing-season trends in key leaf functional traits. Making these connections is key to

understanding the extent to which maps of greendown could be applied in ecological

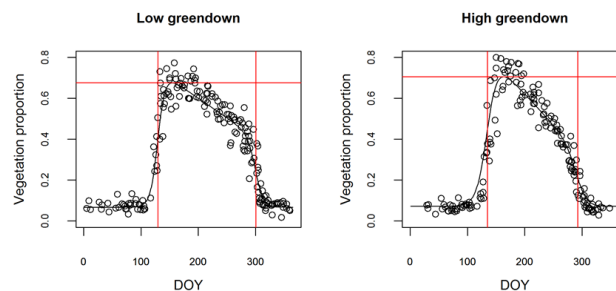research aimed at understanding the response of forest ecosystems to global change.

Figure 1, Examples of a phenology curve of a pixel with low greendown (left) and high greendown (right) at Green Ridge State Forest. The circles represent Landsat data and the solid black line is the fitted greendown-phenology model. The vertical red lines indicate spring onset (left) and autumn offset (right); the horizontal red line indicates maximum vegetation. Greendown is the line (slope) connecting the spring and autumn sigmoid curves resulting in a duel-logistics curve to represent phenology.

Greendown is a measure of declining summer greenness or the rate of change in vegetation reflectance. At the landscape scale, changes in canopy reflectance during the growing season (not including leaf-on and leaf-off) could result from changes in light availability or solar irradiance. Throughout the growing season solar irradiance is influenced by the interaction between sun angle and topography and canopy structure factors that cast shadows (Nunez, 1980), day length (Bauerle et al., 2012) and atmospheric conditions (Flint and Childs, 1987). Topography influences canopy reflectance indirectly by exerting a strong influence over microclimate conditions that control phenology and photosynthetic activity (Dragoni and Rahman, 2012; Fisher et al., 2006; Hwang et al., 2014; Hwang et al., 2011), and influencing species composition (Brown, 1994) and directly by the controlling the amount of sunlight that a location receives (Knyazikhin et al., 2013). In mountainous terrain, lower elevation areas receive less direct solar irradiance in the early and late part of the day because surrounding ridges block sun light (Flint and Childs, 1987; Nunez, 1980). At a finer scale, canopy rugosity influences the degree of inter-canopy shading and albedo (Ogunjemiyo et al., 2005; Parker and Russ, 2004) and therefore the amount of solar irradiance received by individual trees. For example, as the solar zenith angle increases throughout the growing season, high rugosity canopies will exhibit greater shadow effects than low (smooth) rugosity canopies (Asner et al., 2015). These observations lead us to hypothesize that if greendown is related to changes in canopy reflectance as the sun zenith angle increases throughout the growing season then topographic features, rugosity and solar irradiance will explain greendown variance. To test this hypothesis we compared greendown with topographic data and a solar irradiance model generated from GIS data.

Visible (VIS, 400-700 nm) and near infrared (NIR, 750-950nm) reflectance are important measurements for assessing vegetation using remote sensing technology (Ollinger, 2011). Very little NIR light is absorbed by leaves with the majority of NIR scattered or transmitted. Leaf NIR scattering is strongly influenced by leaf structural characteristics such as mesophyll thickness, the ratio of mesophyll surface to intercellular air pockets, cuticle thickness, leaf trichome density, ratio between palisade mesophyll to spongy mesophyll, leaf thickness, geometry, and orientation (Knapp and Carter, 1998; Moorthy et al., 2008; Ollinger, 2011; Slaton et al., 2001). In general, healthy leaves absorb VIS light with the exception of the green wavelength. Leaf reflectance of VIS including wavelengths other than green (i.e., fall leaf colors) is a function of key leaf traits that influence photosynthesis. Color pigments including chlorophyll pigments are rich in nitrogen (Reich et al., 1991; Wilson et al., 2000; Wilson et al., 2001; Xu and Baldocchi, 2003). Changes in leaf nitrogen will follow with a change in pigment concentration and thus VIS reflectance. VIS and NIR are indirectly affected by water content through changes in photosynthesis and leaf structure (Ollinger, 2011; Slaton et al., 2001). Observations that leaf reflectance correlate with plant functional traits lead to the hypothesis that if greendown is a function of leaf reflectance, then greendown will correlate with changes in VIS and NIR reflectance as leaf functional traits change concomitantly throughout the growing season. To test this hypothesis we collected leaf samples between June and August 2014 from a deciduous forest in the mid-Atlantic region and compared rate of change in leaf measurements (including leaf spectra, key leaf functional traits) to greendown.

Site description and Methods

Site description

This study was conducted in Green Ridge State Forest (GRSF), which is located in the Ridge and Valley physiographic province in Allegany County, western Maryland (Figure 2). Two major northeast-southwest orientated ridges run through the middle of the forest. Elevation ranges from 152-m to 610-m. Mean annual temperature is 12 °C and mean annual precipitation is 94 cm (Owenby and Ezell, 1992). Most of the old-growth forest was harvested for timber by the early 1900's. Since the 1960's, GRSF has been a working forest managed for 100-year old even-age oak-hickory forest. The forest is owned and operated by Maryland Department of Natural Resources Forest Service with the exception of private inholdings. Dominant forest tree species are oaks (*Quercus alba, Q. rubra*, *Q. coccinea*, *Q. prinus*) and hickory (*Carya glabra*) with occasional stands of pine (*Pinus strobus*, *P. rigida*, *P. virginiana*).
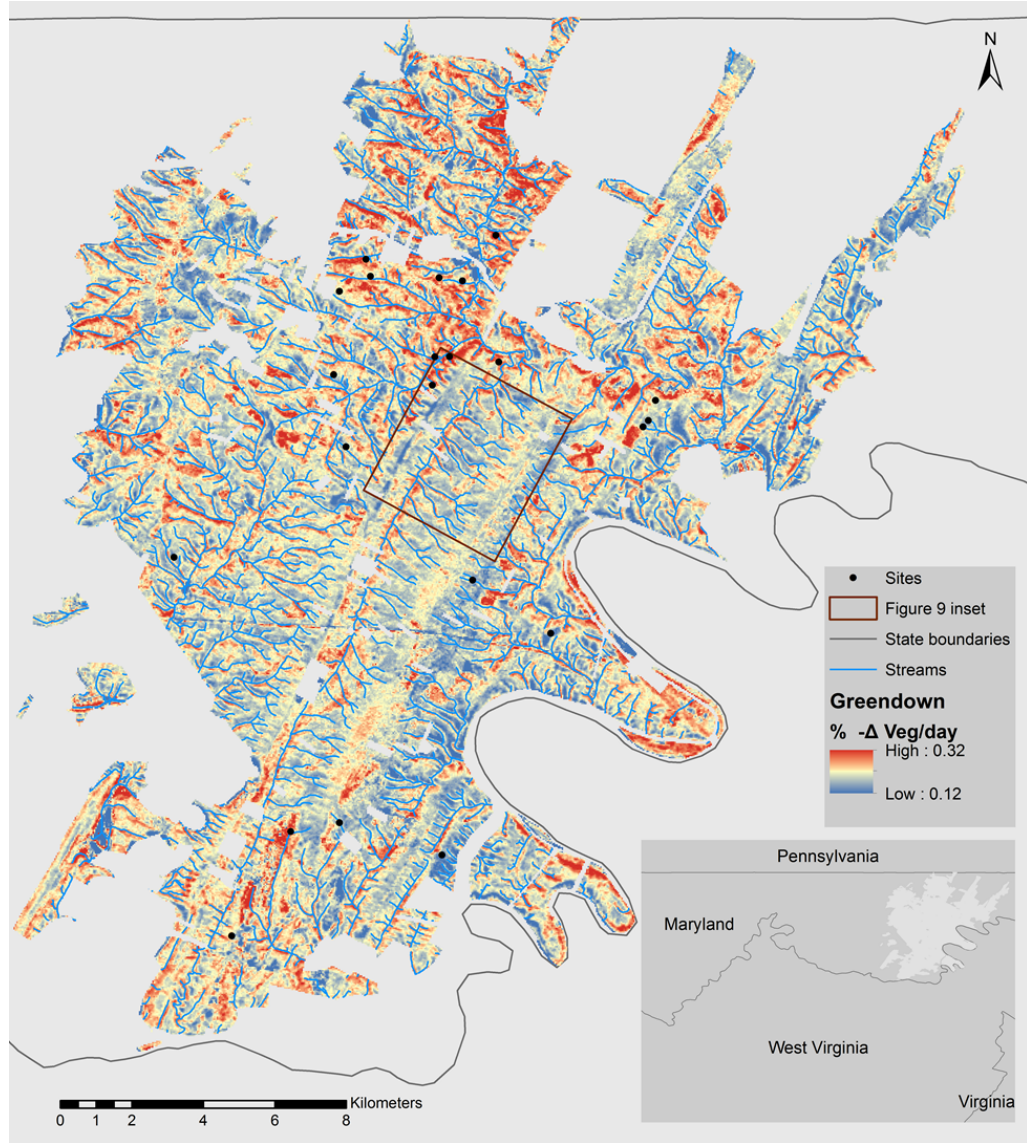
Figure 2. Map of study area in Green Ridge State Forest, along with sites of leaf collection (closed circles) and greendown values. The greendown scale excludes the first and last 2% of its range which were values not typical of interior forest but rather of agriculture fields.

Landsat description and processing

All available atmospherically corrected Landsat TM and ETM+ scenes for path 16/row 33, spanning years 1982-2013, were acquired from the USGS as Climate Data Records (CDR), which are processed using the Landsat Ecosystem Disturbance Acquisition Processing System (LEDAPS) (Masek et al., 2006). LEDAPS provides cloud/cloud shadow masks, which were used to remove pixels with cloud cover. After removing pixels with partial cloud cover the number of observations available for any one location averaged 182 ± 5. A sun-canopy-sensor correction was applied to normalize for topographic effects and differences in sun zenith angle between images (Gu and Gillespie, 1998). Neither the LEDAPS processing nor the sun-canopy-sensor correction adjusts for changes in the bidirectional reflectance distribution function (BRDF) due to changes in vegetation cover throughout the growing season. Linear spectral mixture analysis (SMA) (Adams et al., 1986; Elmore et al., 2000; Smith et al., 1990) was applied using a consistent set of four image-derived endmembers (photosynthetic vegetation (PV), non-photosynthetic vegetation, substrate and shade) to calculate vegetation fraction. This 30+ year record of photosynthetic vegetation fraction (f_{pv}) was organized by day of year to form an average annual time series of f_{pv}, documenting the trajectories of f_{pv} through spring, summer, and autumn.

Fitting phenology curve

The greendown-phenology model ($f_{pv}(t, m) = m_1 + (m_2 - m_7 \cdot t)$

$$\left(\frac{1}{1 + e^{(m_3 - t)/m_4}} - \frac{1}{1 + e^{(m_5 - t)/m_6}} \right)$$ Equation **1**) developed by Elmore et al., (2012) was used to derive average phenology curves fit with Landsat observations of f_{pv} (Figure 1) for all pixels. The left side of equation 1: $f_{pv}(t, \mathbf{m})$, is the SMA-derived

photosynthetic vegetation fraction for time (t, in day of year) corresponding to Landsat scenes. On the right side of the equation, m_1 is the minimum vegetation cover; m_2 is the potential amplitude between m_1 and the maximum vegetation fraction, moderated by m_7, which is greendown. Parameters m_3 and m_5 are the day of year when greenness is most rapidly changing (inflection points on the phenology curve) in spring and autumn. Parameters m_4 and m_6 are related to the rate of spring and autumn changes in f_{pv}, respectively

$$f_{pv}(t, \mathbf{m}) = m_1 + (m_2 - m_7 \cdot t)\left(\frac{1}{1+e^{(m_3-t)/m_4}} - \frac{1}{1+e^{(m_5-t)/m_6}}\right)$$ Equation 1

In the present study, three parameters (m_2, m_3, m_7) were used from the greendown-phenology model. Greendown was rescaled by multiplying it by 100 to arrive at units of percent f_{pv} decline per day (Figure 2). Greendown values for GRSF are representative of greendown values for Allegany County and the entire Landsat image (Figure S1). Negative values of m_7 are extremely rare (1% of GRSF), but represent locations where f_{pv} increased throughout the growing season. Likewise, extreme positive values (>0.6) were less than 1% of GRSF. Pixels at the extreme ends of the greendown range were confined to agriculture fields and barren lands and were thus excluded from further analysis. Interior forest coverage of the Landsat pixels was verified with NAIP imagery in ArcGIS. Greendown was classified into four categories that spanned its range. Within each class, areas that were < 1000m^2 were excluded to eliminate the possibility of establishing sites in the wrong greendown class due to closeness. A total of 21 sites were established within the four classes with an average of 6 sites per class.

Landscape variables

A 2-m digital elevation model (DEM), canopy height model (CHM) and surface model (canopy height + elevation) were generated from a leaf-off LiDAR survey of Allegany County, MD conducted on January 29 and 31, 2012, and February 03, 2012. U.S. Forest Service Fusion software version 3.41 was used for all analyses of the LiDAR survey. Slope and aspect were calculated from the 2-m DEM using eight cell neighbors. Aspect was represented as degrees relative to north (0=north, 180=south, 90 = east or west). Total solar irradiance between June 21 and September 21 was calculated from the surface model using ArcGIS' Area Solar Radiation tool. The solar irradiance calculation required solar zenith angle, DOY and latitude as inputs. The model assumed clear sky conditions, and therefore represents maximum irradiance achievable for each pixel given its topographic position (e.g., valley bottom or ridge position) and canopy structure (degree of inter-canopy shading). For each pixel a 32-m diameter circular neighborhood was used to aggregate the DEM and DEM derived products to match Landsat resolution. Means values of slope, elevation and aspect were used for topographic layers while maximum height was used for canopy height and rugosity was calculated as the standard deviation of canopy height. Total solar irradiance was calculated using the 2-m surface model and resampled to 30-m to match Landsat.

Leaf collection

At each site we collected leaves from *Q. alba*. We focused on *Q. alba* because if the following reasons: (1) it is commonly found throughout GRSF as a dominate species in the upper canopy and was likely to be found throughout the full range of greendown

9

values and (2) to control for potential inter-species variation in leaf-level variables (e.g. N concentration and reflectance values). All sites had three *Q. alba* trees that were present in the upper canopy with the exception of one site which had only one dominate *Q. alba* located in a *Liriodendron tulipifera* stand, a relatively rare species at GRSF. Sunlit canopy leaves were collected from all study trees at 21 sites in June and August 2014. The date of first sampling for each site was approximately 4 weeks after spring onset DOY (m_3; Table S1). This timing meant that sites were exhibiting the same phenophase during the first sampling. Similarly in August, sampling occurred on average 58 days before autumn offset to avoid collecting leaves during the period of rapid senescence. Radiative transfer models suggest there may be a relationship between greendown and rugosity (Garcia-Haro and Sommer, 2002; Hall et al., 1995). To further explore this relationship, a subset of four sites at GRSF was selected for additional sampling in two-week intervals between June and the last sampling in late August. In chronological order these sampling dates will be referred to as early-July, mid-July and early-August. The sites were selected based on a matrix of high and low values for greendown and rugosity. That is each site was one of these greendown and rugosity combinations: (1) high greendown and low rugosity, (2) high greendown and high rugosity, (3) low greendown and high rugosity, (4) low greendown and low rugosity (Table S1).

Leaf samples were collected using a Remington 12 gauge, model 870 express pump action shotgun with a 28" barrel and modified choke and #4 steel shot in 2 ¾" shells with a 1 1/2oz load. The gun operator aimed for a small branch that had a cluster of leaves at the top of the tree canopy. Whenever possible the branches were collected from different sides of the canopy to account for within-canopy variation. Each retrieved

branch was wrapped in a wet paper towel, placed in a labeled zip lock bag or floral water tube and stored in a cooler until processed at the Appalachian Laboratory within five hours of sample collection. One leaf from each branch was selected for analysis, yielding a total of 122 leaf samples for the June and August collection periods. A total of 48 leaf samples were obtained for the early-July and mid-July while early-August had 45 leaf samples collected.

Spectral Measurements

Fresh leaf spectral measurements were performed using an Analytical Spectral Devices Inc. (ASD; Boulder, CO) Fieldspec Pro FR spectrometer (350-2500 nm range). Viewspec Pro version 4.05 was used to post process the spectra, including a spline correction to account for gain differences between the first and second detector. An area of the leaf that was at least 2-cm in diameter and had the least amount of visible damage was chosen for the spectral measurement. Spectral measurements were taken three times and averaged for each measured leaf sample. To maximize comparability with Landsat 7 ETM+ observations we calculated mean leaf reflectance in two wavelength regions: VIS-red (band 3, 0.63-0.69 mm) and NIR (band 4, 0.77-0.90 mm). These two Landsat 7 ETM +bands are strong measurements of vegetation cover and are used to calculate the normalized difference vegetation index (NDVI), a widely used remote sensing index for greenness (photosynthetic capacity) (NIR-VIS-red)/(NIR+VIS-red) (Tucker, 1979). NDVI was calculated using leaf VIS-red and NIR. To measure chlorophyll content, we used the derivative of the red edge (λRE) (λ**max**($dR/d\lambda$)   Equation **2**) generally between 704-726 nm. λRE is used as a reflectance index for chlorophyll

content because of the strong positive relationship between chlorophyll and λRE (Curran et al., 1995; Dillen et al., 2012).

$$\lambda_{max} (dR/d\lambda)$$ Equation 2

Leaf Traits and Isotope Analysis

We used foliar measurements of $\delta^{13}C$ and %N to track changes in leaf functionality throughout the growing season. $\delta^{13}C$ has been shown to be a useful proxy for water stress in leaves (Seibt et al., 2008). Likewise, foliar %N has been used as a useful proxy for productivity due to its role in photosynthesis. I.e, rubisco and chlorophyll both important for photosynthesis are rich in nitrogen (Reich et al., 1991; Wilson et al., 2000). Each of these leaf constituents could potentially influence leaf reflectance or likewise correlate with canopy structural changes throughout the growing season that influence greendown. For example, a relationship between VIS and %N is expected due to the fact that mechanisms important to photosynthesis (i.e., chlorophyll concentration) also influence VIS reflectance are rich in nitrogen. While there is no direct mechanism linking %N and NIR reflectance, there is an inverse correlation between N and NIR in deciduous leaves (Bartlett et al., 2011; Sullivan et al., 2013).

A 2-cm wide leaf section (the same section

Statistical Analysis

$$c0 + civi$$ Equation **3**) with model effects of maximum vegetation, elevation, slope, aspect, rugosity and solar irradiance was developed to test how well these variables explained greendown (response variable).

$$Greendown = c_0 + \sum c_i v_i$$ Equation 3

C_0 is the intercept, ci is the coefficient and vi is equal to MaxVeg, elevation, slope, aspect, irradiance and rugosity. A multiple linear regression was performed on the model (model 1). Six subsequent models iteratively removed one model effect (model 2-7, Table 1). Additionally, an ANOVA was performed on all models to determine percent variance of each model effect. Maximum vegetation (MaxVeg) is derived from the greendown-phenology model and is the maximum of equation 3. Elmore et al., (2012) found a strong correlation between MaxVeg and greendown (r = 0.61) similarly, we too observed a strong correlation (r=0.45) and thus concluded that even in the absence of landscape variability model parameters MaxVeg and greendown will correlate. Therefore, we deemed it necessary to include MaxVeg in our linear landscape model in explaining greendown variance. Percent variance explained by each model effect was calculated from ((sum squares$_{\text{model effect}}$/ (model-residuals + sum squares$_{\text{model effect}}$) x 100).

To further investigate the relationship between greendown and topographic variables (elevation, slope and aspect) each variable was divided into four quantiles (x_n) and correlations between greendown and the other two topographic variables were conducted in each quantile. This was also done with solar irradiance to understand how interactions between two landscape variables influenced solar irradiance. That is, for landscape variable (a) in quantile (a_n), a Pearson correlation and one-way ANOVA was conducted for landscape variable (b) and landscape variable (c) with greendown and separately with solar irradiance.

Leaf-level measurements were averaged to each site to avoid pseudo replication. Delta (Δ) is the difference between August and June mean leaf value for each leaf variable (i.e., Δ-VIS). A Pearson correlation was performed for the Δ-VIS, Δ-NIR, Δ-

NDVI and Δ-λRE with greendown; and Δ-VIS, Δ--NIR, Δ-NDVI, Δ-λRE and greendown with δ^{13}C and %N. An ANOVA was used to test if the mean values between June and August leaf variables were significantly different. Boxplot figures of temporal trends for all leaf variables are in Appendix I.

Results

Landscape variables

Among the seven models tested, three (models 1, 3 and 7) had an $R^2=0.47$ (Table 1). Maximum vegetation (MaxVeg) explained >25% of greendown variance for all models in which MaxVeg was included. Aspect and elevation consistently explained between 10-18% of greendown variance with the exception of model 2, which excluded MaxVeg and had the lowest R^2 value (0.2). To further test the importance of elevation and aspect in explaining greendown variance, the residuals from model 4 ($R^2=0.40$; excluded aspect) and model 5 ($R^2=0.39$; excluded elevation) were plotted against aspect and elevation, respectively (Figure 3). The large decrease in greendown variance explained by elevation when MaxVeg was excluded (model 2) indicated a collinearity between the model effects. A Pearson Correlation revealed a strong positive correlation (r =0.29, p <0.001; Figure 4).

	Units	% Model Sum Squared Variance						
		model1	model2	model3	model4	model5	model6	model7
Intercept	% Δ Veg d^{-1}	**8.80**	**31.33**	**12.04**	**7.17**	**9.45**	**4.17**	**9.81**
MaxVeg	% Veg	**33.86**	-	**33.24**	**31.70**	**25.54**	**33.27**	**33.54**
Slope	% grade	1.21	0.28	-	1.25	1.43	2.42	1.41
Aspect	degree	**12.45**	**9.58**	**12.49**	-	**9.08**	**14.40**	**13.27**
Elevation	m	**13.42**	**2.53**	**13.61**	**10.09**	-	**17.98**	**14.30**
Sol Irrad.	WH/m^2	**4.86**	**4.00**	**6.03**	**6.97**	**9.87**	-	**4.98**
Rugosity	Std (m)	**0.83**	0.34	**1.04**	**1.76**	**1.83**	**0.96**	-
Model R^2		**0.47**	**0.20**	**0.47**	**0.40**	**0.39**	**0.45**	**0.47**

Table 1. Greendown variance explained by each model effect and modeled r^2 values for each linear model. Bold indicates significance (p <0.05). Dashed line (-) indicates model effect was excluded from the model.
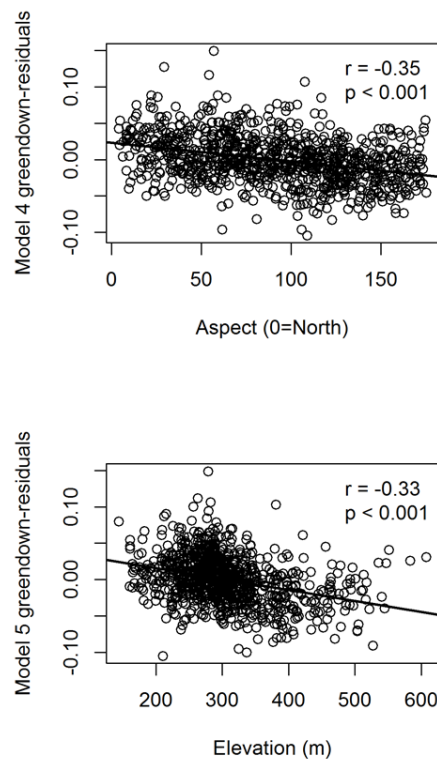

Figure 3. Pearsone Correlation of model 4 greendown-residuals vs, aspect (top) and model 5 greendown-residuals vs elevation (bottom).
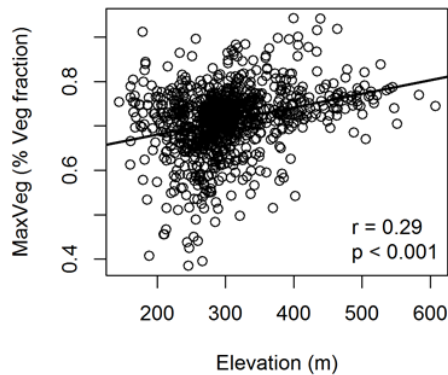
Figure 4. Pearson Correlation between MaxVeg and elevation

A Pearson Correlation indicated that aspect and greendown had a correlation between -0.2 to -0.4 in all slope and elevation quantiles (Table 2). An ANOVA revealed that aspect explained between 4 and 19% of greendown variance among slope and elevation quantiles. In the aspect quantiles, elevation correlated with greendown with an r = -0.2 to -0.3 and explained 3-8% of greendown variance. Slope and greendown correlated with an r=0.3 and explained 8% variance in the south facing aspect quantile. Landscape quantiles and the relationship with solar irradiance yielded similar results (Table 3). Negative correlations between solar irradiance and slope were exhibited in aspect and elevation quantiles with the strongest negative relationship in the south facing aspect (r=-0.32) with slope explaining 10% of solar irradiance variance in south facing aspects. In south and south-east/west facing aspect quantiles, elevation was positively correlated with solar irradiance (r=0.5 and 0.4), and elevation explained between 16-25% of solar irradiance variance. There was a general trend of lower solar irradiance within

quantiles with higher rates of greendown. A Pearson Correlation revealed a negative

correlation (p = -0.31, p< 0.001) between solar irradiance and greendown (Figure 5).

Landscape var. A	Landscape var. B				Landscape var. B			
Elevation quantiles	Slope vs. Greendown				Aspect vs. Greendown			
	r	p	% SS	P (>F)	r	p	% SS	P (>F)
Elev> 260	0.02	0.82	0.02	0.8222	**-0.3**	**<0.001**	**10.52**	**<0.001**
260< Elev <294	**0.16**	0.013	**2.60**	**0.0134**	**-0.4**	**<0.001**	**18.83**	**<0.001**
294< Elev<334	**0.15**	0.025	**2.14**	**0.0250**	**-0.3**	**<0.001**	**7.87**	**<0.001**
Elev >334	0.08	0.23	0.62	0.2303	**-0.3**	**<0.001**	**10.25**	**<0.001**
Aspect quantiles	Slope vs. Greendown				Elevation vs. Greendown			
	r	p	% SS	P (>F)	r	p	% SS	P (>F)
South	**0.32**	**<0.001**	**8.03**	**<0.001**	**-0.3**	<0.001	**8.03**	**<0.001**
S-East/West	0.09	0.15	5.41	0.1535	**-0.2**	<0.001	**5.41**	**<0.001**
N-East/West	0.06	0.35	7.80	0.3513	**-0.3**	<0.001	**7.80**	**<0.001**
North	0.04	0.55	2.92	0.5541	**-0.2**	0.0086	**2.92**	**<0.001**
Slope quantiles	Aspect vs. Greendown				Elevation vs. Greendown			
	r	p	% SS	P (>F)	r	p	% SS	P (>F)
Flat	**-0.21**	**0.002**	**4.23**	**0.002**	**-0.3**	**<0.001**	**7.00**	**<0.001**
10< Slope <15	**-0.28**	**<0.001**	**7.72**	**<0.001**	**-0.2**	**<0.001**	**5.78**	**<0.001**
15< Slope <21	**-0.33**	**<0.001**	**11.21**	**<0.001**	**-0.2**	**0.019**	**2.34**	**0.012**
Steep	**-0.38**	**<0.001**	**14.50**	**<0.001**	**-0.2**	**0.015**	**2.52**	**0.015**

Table 2, Landscape variables (elevation, slope and aspect) binned by quantiles. Within each quantile a Pearson correlation and ANOVA was performed on the other two landscape variables with greendown to identify interaction affects. Bold indicates significance (p <0.05).

Landscape var A	Landscape var B				Landscape var B			
Elevation quantiles	Slope vs. Solar Irradiance				Aspect vs. Solar Irradiance			
	r	p	% SS	Pr(>F)	r	p	% SS	Pr(>F)
Elev> 260	-0.28	<0.001	7.76	<0.001	0.28	<0.001	7.71	<0.001
260< Elev <294	-0.24	<0.001	5.88	<0.001	0.25	<0.001	6.41	<0.001
294< Elev<334	-0.19	<0.001	3.73	0.003	0.076	<0.001	0.58	0.243
Elev >334	-0.043	<0.001	0.19	0.511	-0.17	<0.001	2.88	0.009
Aspect quantiles	Slope vs. Solar Irradiance				Elevation vs. Solar Irradiance			
	r	p	% SS	Pr(>F)	r	p	% SS	Pr(>F)
South	-0.32	<0.001	10.34	<0.001	0.5	<0.001	24.97	<0.001
S-East/West	-0.12	<0.001	1.51	0.060	0.4	<0.001	16.28	<0.001
N-East/West	-0.25	<0.001	6.32	<0.001	0.11	<0.001	1.24	0.088
North	-0.22	<0.001	4.90	<0.001	0.044	<0.001	0.19	0.501
Slope quantiles	Aspect vs. Solar Irradiance				Elevation vs. Solar Irradiance			
	r	p	% SS	Pr(>F)	r	p	% SS	Pr(>F)
Flat	0.1	<0.001	1.04	0.119	0.14	<0.001	1.88	0.035
10< Slope <15	0.028	<0.001	0.08	0.666	0.22	<0.001	4.91	<0.001
15< Slope <21	0.084	<0.001	0.70	0.200	0.34	<0.001	11.30	<0.001
Steep	0.088	<0.001	0.77	0.180	0.33	<0.001	10.67	<0.001

Table 3. Landscape variables (elevation, slope and aspect) binned by quantiles. Within each quantile a Pearson correlation and ANOVA was performed on the other two landscape variables with solar irradiance to identify interaction affects. Bold indicates significance (p <0.05).
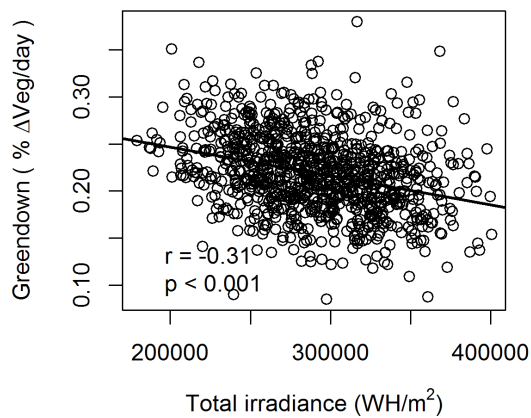

Figure 5. Pearson Correlation between greendown and total solar irradiance.

Leaf-level variables

There were no correlations between greendown and Δ-VIS-red, Δ-NIR, Δ-NDVI, Δ-λRE, or with Δ-VIS-red, Δ-NIR, Δ-NDVI, Δ-λRE (Figure 1, Table 4). A Pearson correlation revealed a positive relationship between Δ-VIS-red, Δ-NIR and Δ- δ^{13}C (p≤ 0.05) (Figure 7, Table 4). A one-way ANOVA between June and August means revealed VIS-red reflectance and subsequently NDVI were the only variables significantly different from one another (Figure 1, Figure S2). NIR and NDVI steadily decreased throughout the growing season whereas λRE increased (Figure S3). VIS-red reflectance appeared constant between early July and early August then increased in late August. Between June and early August leaf carbon increased while nitrogen decreased before both increasing in late August (Figure S4).Throughout the sampling periods δ^{13}C became more negative.
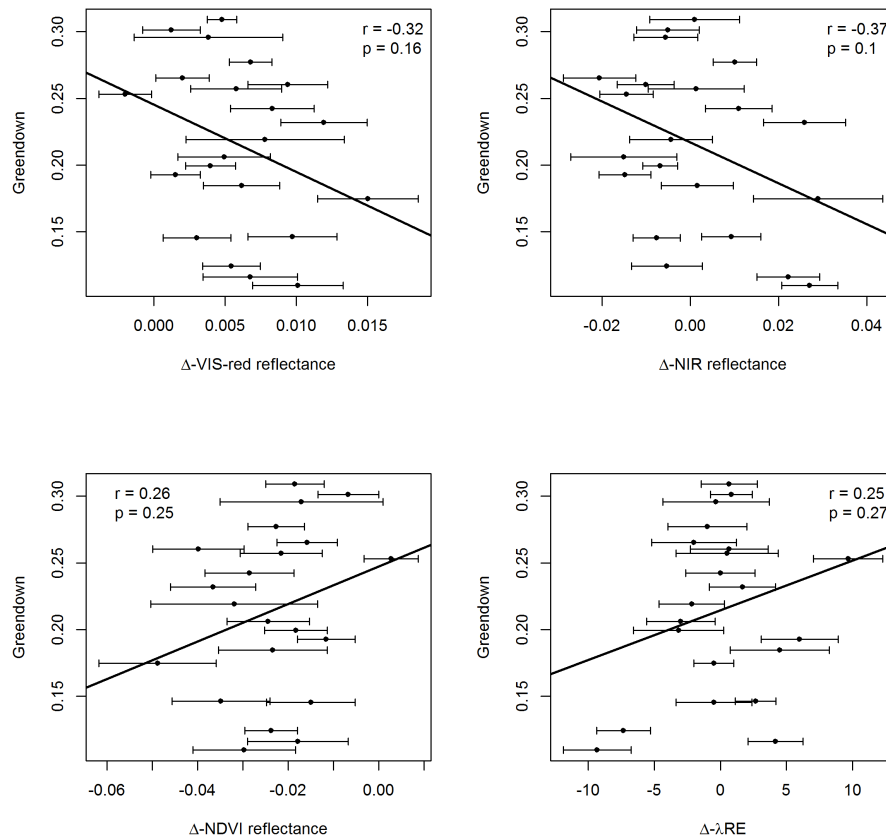
Figure 6. Pearson correlation between greendown and leaf Δ: VIS, NIR, NDVI and λRE. Delta was calculated as variable(August –June). Positive Δ indicates August value was higher than June value. Δ: VIS, NIR, NDVI are in units of reflectance while Δ-λRE is nm and greendown is (% Δ-Veg/day). Error bars for Δ-leaf variable are the standard error for August and June added with quadrature. Elmore et al., (2012) calculated 95% uncertainty intervals of ± .07 for greendown.
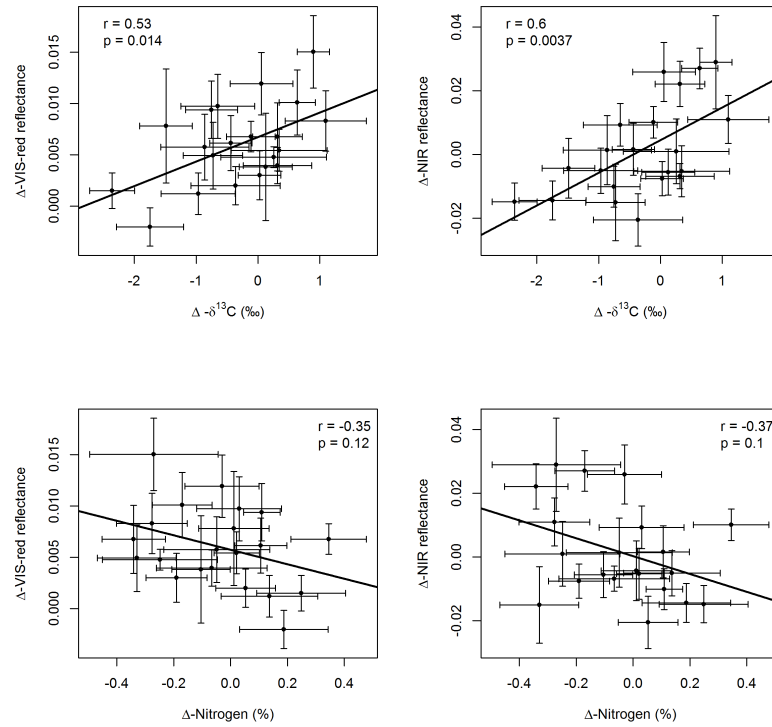
Figure 7. Pearson correlation between leaf Δ-VIS-RED and Δ-NIR with Δ-δ^{13}C and Δ-N. A positive Δ for δ^{13}C indicates that August was less negative (more water stressed) compared to June. Error bars for Δ-leaf variable are the standard error for August and June added with quadrature.

	C	δ13C	N	δ15N	Greendown
VIS-red	0.16	**0.53**	-0.35	-0.26	-0.32
NIR	-0.047	**0.6**	-0.37	0.36	-0.37
NDVI	0.2	-0.43	0.29	0.17	0.26
λRE	**0.51**	-0.52	0.3	-0.13	0.25

Table 4. Pearson correlation for greendown and leaf variables. August and June-August. Bold indicates significance (p<0.05)
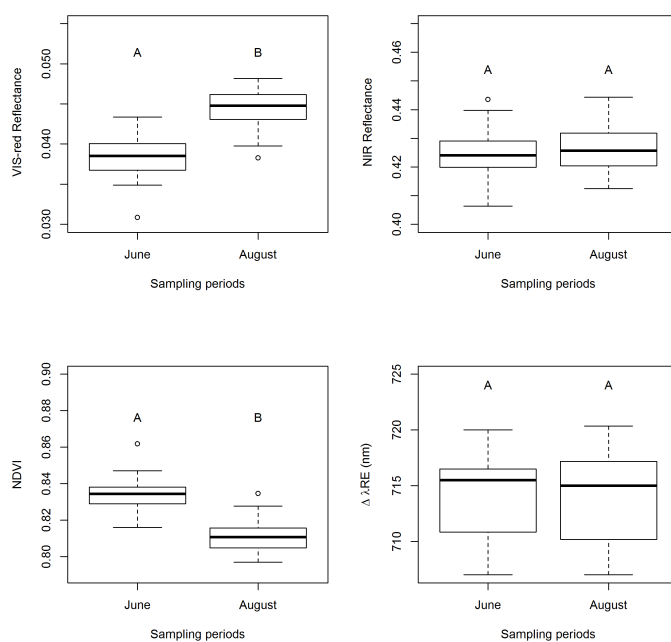

Figure 8. Boxplots of June and August VIS-red, NIR, NDVI and λRE mean values. Letters indicate a significant difference between June and August determined by a one-way ANOVA.

Discussion

Landscape variables

We first hypothesized that topographic factors (elevation, slope, aspect) and canopy structure (rugosity) would influence the change in incident solar irradiance experienced by canopies throughout the growing season, and would therefore have an effect on greendown. A visual comparison of each landscape factor with greendown suggested the hypothesized spatial patterns (Figure 7). A linear model with all landscape factors and MaxVeg as model effects supported our hypothesis and explained nearly 50% of greendown variance ($R^2 = 0.47$, $p < 0.001$). Aspect explained the greatest proportion of model variance, demonstrating that sites facing away from the solar incident angle (i.e., north-facing sites) experience the strongest greendown. At these sites, the greater solar zenith angle experienced as the vernal equinox approaches produces greater shadowing and therefore a greater reduction in NIR reflectance relative to south-facing sites. Interactions between slope, elevation, and aspect supported the conclusion that topographic position influences greendown. For example, the effect of aspect on greendown increased with increasing slope. Slope and elevation were weakly correlated with greendown and solar irradiance on north-facing slopes that experience significant shadowing. On south-facing aspects where shadowing is less extensive, slope exhibited a stronger negative correlation with solar irradiance and positive correlation with greendown, whereas elevation was positively correlated with solar irradiance and negatively correlated with greendown. Thus, aspect influences the strength of slope and elevation effects on solar irradiance and greendown.

We found that rugosity, a measure of canopy complexity, explained less than 2% of greendown variance in all models, and was therefore not a useful metric for understanding landscape-level variation in how sun incident angle interacts with canopies to determine greendown. Conceptually, effects of shadowing due to topographic position are modified by canopy complexity that enhances inter-canopy shadowing within Landsat pixels and should therefore also influence greendown. There are several studies that demonstrate that canopy structural changes following forest disturbance are associated with changes in shadow fraction within Landsat pixels (Asner et al., 2015; Hardy et al., 2004; Li and Strahler, 1992; Panferov et al., 2001; Sabol et al., 2002). Radiative transfer models also suggest that increasing canopy complexity creates more shadows as the solar zenith angle decrease throughout the growing season (Essery et al., 2008; Garcia-Haro and Sommer, 2002; Hall et al., 1995). Therefore, areas with higher rugosity are expected to have higher greendown. Finally, studies have demostrated that canopy structure greatly influences NIR scattering in canopies (Asner and Martin, 2008; Asner et al., 2015; Craine et al., 2009; Knyazikhin et al., 2013). Thus, although canopy structure influences canopy incident solar radiation and NIR reflectance, our results suggest that at the landscape scale topographic factors exert a stronger influence over incident solar irradiance than canopy structure. Given the strong effect of topography, perhaps it is unrealistic to expect detection of the relatively smaller contribution from canopy structure.

Elevation and aspect, shown here to correlate with greendown, also influence phenology through their control on temperature and moisture gradients (Dragoni and Rahman, 2012; Fisher et al., 2006; Fridley, 2009; Hwang et al., 2014); knowledge of how topography influences phenology might provide some further insight into the relationship

of greendown and topography. For example, leaf-on and leaf-off dates correlate with elevation (Moser et al., 2010; Tateno et al., 2005; Vitasse et al., 2009). Aspect greatly influences potential evapotranspiration and solar irradiance (Holland and Steyn, 1975; Perry et al., 2008) influencing nutrient dynamics and productivity (Grant, 2004). Jackson (1966) found that plants on north-facing slopes tended to flower later than their south-facing counterparts at the same elevation. It is important to acknowledge that factors that contribute to phenology might also affect the degree of greendown. For instance, temperature gradients associated with leaf-off might also influence greendown. Elevation and aspect tended to explain a greater percent of greendown variance than solar irradiance (Tables 2 and 3) which highlights the fact that microclimate conditions associated with elevation and aspect might also be important determinants of canopy structure and therefore reflectance. Future research should improve these models by including average climate data with landscape variables to fit the temporal resolution of average Landsat phenology. Species composition also varies along topographic gradients (Trimble and Weitzman, 1956). For example, a study done in the central Appalachian mountains found that *Q alba, Quercus velutina* and *Nyssa sylvatica* had a preference for southwest facing aspect while *Acer saccharum, Liriodendron tulipifera* and *Prunus serotine* were mostly found on north facing aspect (Desta et al., 2004). Greendown is primarily driven by decline in NIR reflectance through the growing season, and NIR is influenced by leaf structure, which varies across species. Thus, NIR and greendown signals could be influenced by species composition along topographic gradients. Topographic effects on radiance were accounted for in the present study but changes in BRDF due to changes in phenology have not been addressed in pre and post-processing

26

corrections for Landsat data. However, changes in BRDF due to phenology may be more
of a factor at the beginning and end of the growing season than during the growing
season because BRDF between soil and vegetation are dramatically more different than
from changes in vegetation. Therefore not correcting for BRDF due to changes in
phenology is not a major concern for NIR or greendown measurements from Landsat.
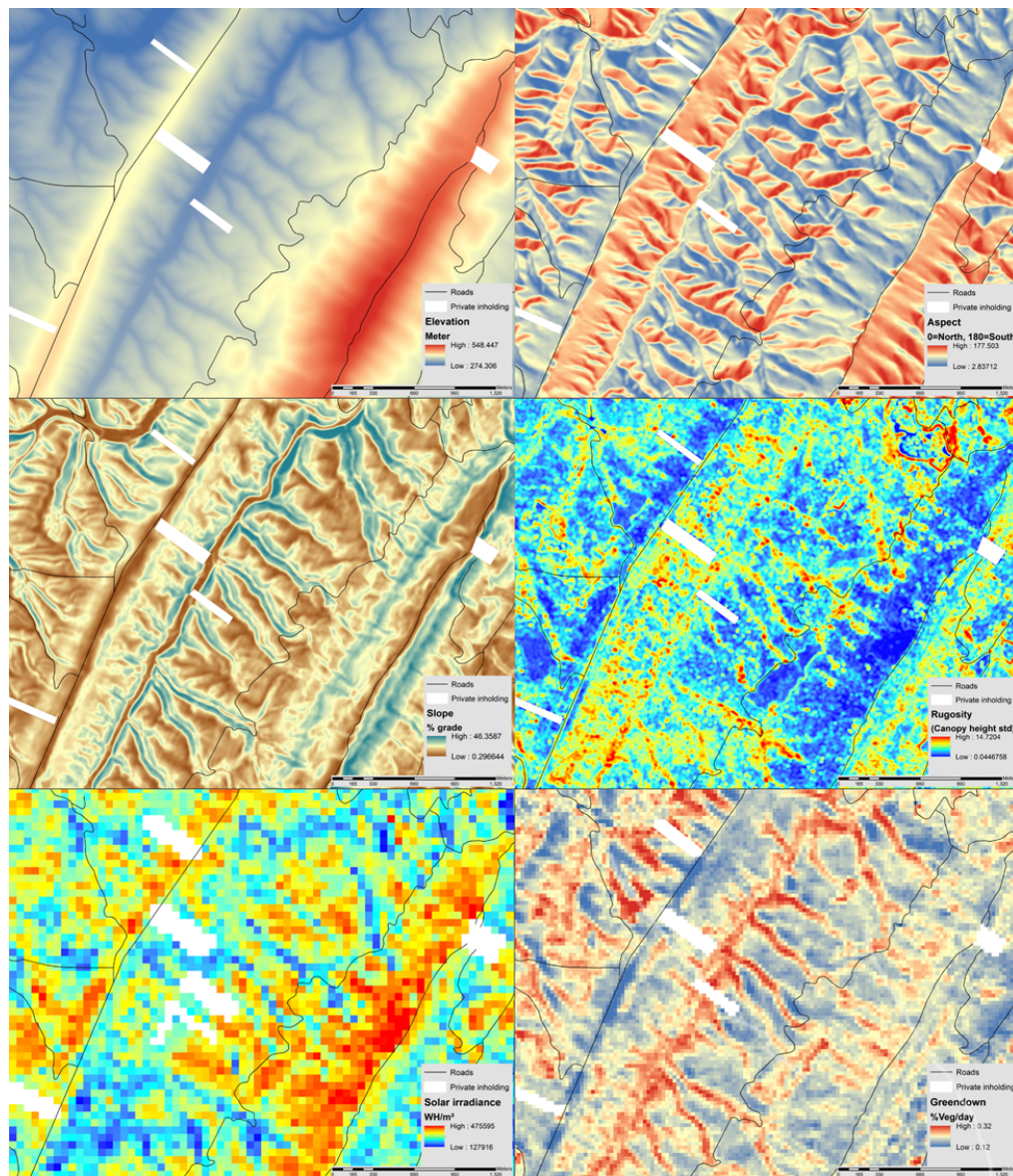

Figure 9. Close-up of landscape variables and greendown at Green Ridge State Forest.

Leaf-level variables

Our second hypothesis posits that greendown is a function of changes in leaf reflectance, which are concomitant with changes in leaf functional traits throughout the growing season. Leaf reflectance measurements did not trend consistently in one direction through the growing season. Leaf-level measurements of VIS-red reflectance increased throughout the growing season and June and August means were significantly different (R^2=0.54, p <0.001). However, mean leaf NIR reflectance measurements were indistinguishable between June and August. These observations were similar to measurements of key leaf traits and spectra reported in previous studies of leaf reflectance (Keenan et al., 2014; Wilson et al., 2001; Yang et al., 2014), however, there were some contrasting results. A time series of *Q. alba* leaf spectra from Yang et al (2014) detected much more variability within the growing season and exhibited increasing visible reflectance and decreasing near infrared reflectance. Similar to Wilson et al., (2001) we detected a declining trend in foliar N concentration, while, Keenan et al., (2014) and Yang et al., (2014) reported constant foliar N for *Quercus rubra* and *Q. alba* over a growing season. One possibility for why N and spectral trends differed between Yang et al., (2014) and Keenan et al., (2014) to Wilson et al., (2000) and our study is ectopic variation driven by local adaptation to environmental differences between locations. Keenan et al., (2014) and Yang et al., (2014) studies were both conducted in Massachusetts while Wilson et al., (2000) and our study was done in southern Appalachian forests. Oaks in southern Appalachia are better adapted to drought conditions than oaks in New England because of a decrease in precipitation going southward along the latitudinal gradient. Oaks are anisohydric, meaning oaks lower their

water potential to maintain a constant stomatal conductance (keep stomates open) during drought. If oaks in southern Appalachia are more drought adapted and therefore exhibit a stronger ansiohydric behavior than oaks in New England then differences in leaf functionality and reflectance would be observed between oaks in the two different regions.

Despite the lack of consistent trends in leaf reflectance (particularly NIR reflectance), we did find that changes in leaf reflectance correlated with some measured leaf traits. For example, positive correlations between leaf $\Delta - \delta\ ^{13}C$ and changes in leaf reflectance (Δ-VIS-RED and Δ-NIR) support findings of previous research (Bowman, 1989) on the increase in leaf reflectance caused by plant water stress. A positive change in $\Delta - \delta\ ^{13}C$ indicated that trees were more water stressed in August than in June; our results revealed a positive correlation between $\Delta - \delta\ ^{13}C$ with an increase in VIS-red and NIR reflectance. In the short term, water stress affects VIS reflectance by limiting photosynthesis through the closure of stomates. If stomates close then less energy is captured to maintain an energy balance in the leaf between light captured and light used for sugar production (Gimenez et al., 1992). Long term effects of water stress will result in a decrease in photosynthetic mechanisms, structural changes, leaf damage and leaf mortality (Shao et al., 2008). Water stress effects NIR by effecting leaf structure, for example, a decrease in mesophyll thickness induced by water stress will decrease NIR reflectance (Chartzoulakis et al., 2002).

Leaf reflectance was correlated with variation in leaf functional traits (primarily changes in d13C), but these variables did not exhibit unidirectional trends through time. Thus, it is perhaps not surprising that the measured leaf variables (Δ-$\delta^{13}C$, Δ-N, Δ-C, Δ-

29

δ^{15}N) were not correlated with greendown. With no observable correlations between leaf reflectance and changes in the measured leaf functional traits with greendown we conclude that greendown is not an appropriate tool to track changes in these leaf-functional traits. While our two hypotheses are not mutually exclusive, it is apparent that NIR scattering due to interactions between topographic position, canopy structure, and sun angle provide far greater variability to the Landsat reflectance signal than do leaf chemical or leaf reflectance signals. This is consistent with research reporting a mismatch between leaf biochemistry and canopy reflectance derived from hyperspectral remote sensing data due to the influence of canopy structure on NIR scattering (Asner and Martin, 2008; Asner et al., 2015; Craine et al., 2009; Knyazikhin et al., 2013). Future research on this topic should include rectifying NIR scattering due to canopy structure and test whether greendown might be correlated with changes in leaf functional traits after accounting for topographic and canopy structure effects.

Conclusion

We found that greendown variance is partially explained by landscape features with elevation, aspect and solar irradiance being the greatest influences, and to a lesser extent rugosity and slope. Additionally, we observed that greendown and solar irradiance were not linearly correlated with any single landscape variable because of interactions among elevation, slope and aspect. We used a relatively simple model of solar irradiance in an attempt to integrate the interacting effects of topographic factors, however, we did not address mechanistic relationships between topography, climate. Future studies might find it fruitful to further explore these relationships. Greendown is not an appropriate tool to measure changes in key leaf functional traits. However, previous research suggests that

30

NIR scattering from canopy structure overwhelms the leaf-reflectance signal. If future

research is able to effectively integrate canopy structure within reflectance models,

greendown might prove useful in tracking residual variance in canopy reflectance related

to leaf reflectance and functional traits. A greater understanding of how greenness

changes throughout the growing season may improve the applicability of Landsat

phenology in climate change research and ecosystem models that incorporate phenology

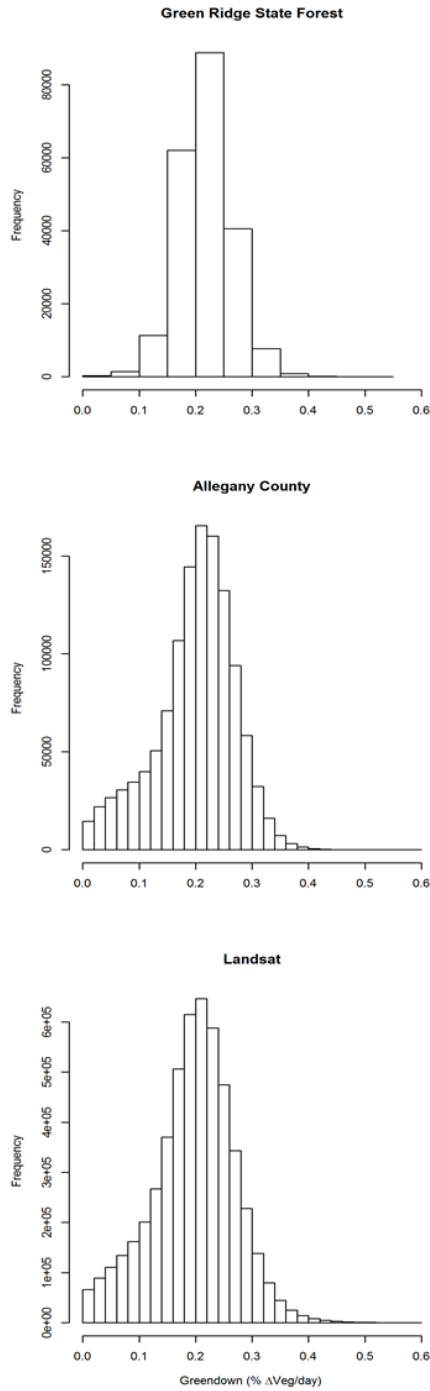to calculate carbon fluxes, energy balance and water budgets.

Appendix I

Figure S1. Frequency of greendown values for Green Ridge State Forest, Allegany County and the Landsat images (path 16/row 33).

Sites	Spring Onset (SO) DOY	Sampled (S) DOY	Δ (SO DOY- S DOY)
6H2[*]	124.79	153	28.21
6H3	125.06	154	28.94
6L6[*]	129.62	156	26.38
6M2	128.95	154	25.05
6M3	133.34	165	31.66
7H1	126.27	156	29.73
7H2	128.05	155	26.95
7H3	133.43	160	26.57
7L1	131.71	162	30.29
7L2	139.07	165	25.93
7M3	127.36	156	28.64
7M7	140.04	171	30.96
8H6	138.20	168	29.80
8H9	141.05	171	29.95
8L2	141.61	169	27.39
8L5	141.76	169	27.24
8M3	137.41	168	30.59
8M4	131.56	162	30.44
9H3	130.64	160	29.36
9H5[*]	140.03	171	30.97
9L3[*]	134.71	169	34.29
9M5	138.50	169	30.50

Table S1. List of sites, spring onset (m_3), date sampled and the time difference between m_3 and date sampled. The first number for the site name denotes a categorical value for greendown between 6 and 9 with 6 being low greendown and 9 being high greendown. The letter denotes a rugosity value: L=low, M=medium, H-High. The last number indicates which replicate site out of potential sites selected before site establishment. [*] Sites selected for additional sampling between the June and August campaign.
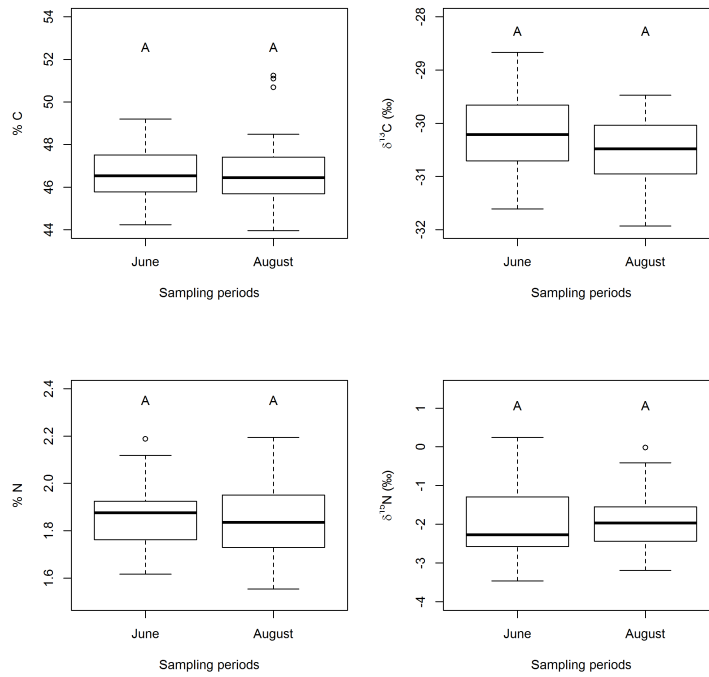
Figure S2: Boxplot of %C, δ^{13}C, %N, and δ^{15}N during June and August. Letters indicate a significant difference between June and August was significant.
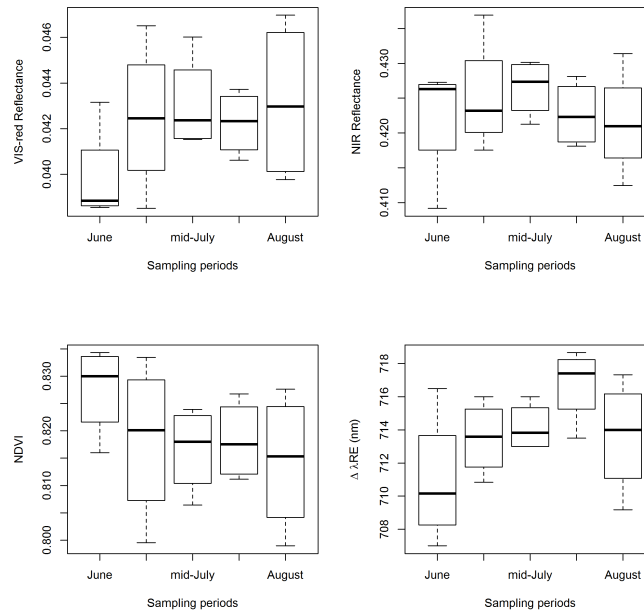

Figure S3. Boxplot of VIS-red, NIR, NDVI and λRE means for the four subset sites in for all five sampling campaigns: June, early-July, mid-July, early-August and August. It should be noted that during early-August sampling 3 samples at site 6L6 were not attained.

Figure S4. Boxplot of %C, δ^{13}C, %N, and δ^{15}N means for the four subset sites in for all five sampling campaigns: June, early-July, mid-July, early-August and August. It should be noted that during early-August sampling 3 samples at site 6L6 were not attained.
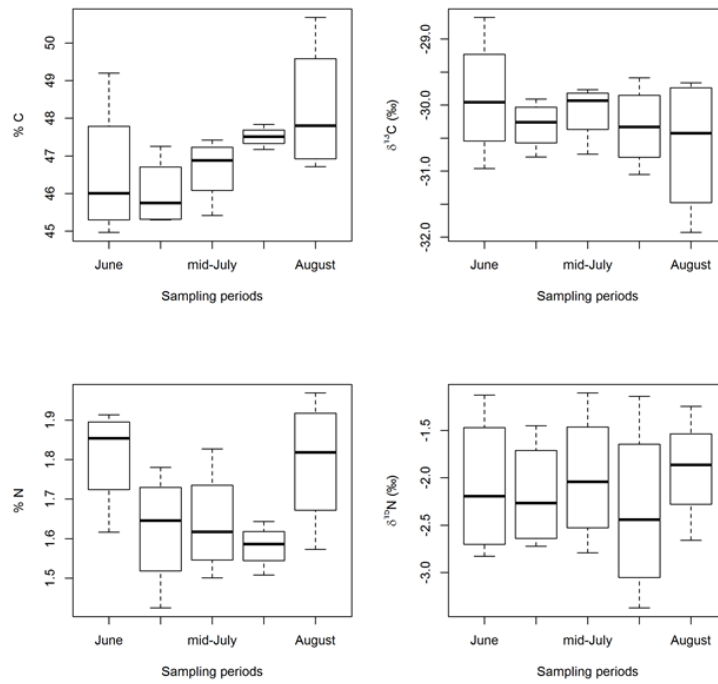
Literature Cited

Adams, J.B., Smith, M.O. and Johnson, P.E., 1986. Spectral mixture modeling: A new analysis of rock and soil types at the Viking Lander 1 Site. Journal of Geophysical Research-Solid Earth and Planets, 91(B8): 8098-8112.

Asner, G.P. and Martin, R.E., 2008. Spectral and chemical analysis of tropical forests: Scaling from leaf to canopy levels. Remote Sensing of Environment, 112(10): 3958-3970.

Asner, G.P., Martin, R.E., Anderson, C.B. and Knapp, D.E., 2015. Quantifying forest canopy traits: Imaging spectroscopy versus field survey. Remote Sensing of Environment, 158: 15-27.

Bartlett, M.K., Ollinger, S.V., Hollinger, D.Y., Wicklein, H.F. and Richardson, A.D., 2011. Canopy-scale relationships between foliar nitrogen and albedo are not observed in leaf reflectance and transmittance within temperate deciduous tree species. Botany, 89(7): 491-497.

Bauerle, W.L. et al., 2012. Photoperiodic regulation of the seasonal pattern of photosynthetic capacity and the implications for carbon cycling. Proceedings of the National Academy of Sciences of the United States of America, 109(22): 8612-8617.

Bonan, G.B., 2008. Forests and climate change: Forcings, feedbacks, and the climate benefits of forests. Science, 320(5882): 1444-1449.

Bowman, W.D., 1989. The relationship between leaf water status, gas exchange, and spectral reflectance in cotton leaves. Remote Sensing of Environment, 30(3): 249-255.

Brown, D.G., 1994. Predicting vegetation types at treeline using topography and biophysical disturbance variables. Journal of Vegetation Science: 641-656.

Chartzoulakis, K., Patakas, A., Kofidis, G., Bosabalidis, A. and Nastou, A., 2002. Water stress affects leaf anatomy, gas exchange, water relations and growth of two avocado cultivars. Scientia Horticulturae, 95(1-2): 39-50.

Cleland, E.E., Chuine, I., Menzel, A., Mooney, H.A. and Schwartz, M.D., 2007. Shifting plant phenology in response to global change. Trends in Ecology & Evolution, 22(7): 357-365.

Cook, B.I., Wolkovich, E.M. and Parmesan, C., 2012. Divergent responses to spring and winter warming drive community level flowering trends. Proceedings of the National Academy of Sciences of the United States of America, 109(23): 9000-9005.

Craine, J.M. et al., 2009. Global patterns of foliar nitrogen isotopes and their relationships with climate, mycorrhizal fungi, foliar nutrient concentrations, and nitrogen availability. New Phytologist, 183(4): 980-992.

Curran, P.J., Windham, W.R. and Gholz, H.L., 1995. Exploring the relationship between reflectance red edfe and chlorophyll concentration in slash pine leaves. Tree Physiology, 15(3): 203-206.

Desta, F., Colbert, J.J., Rentch, J.S. and Gottschalk, K.W., 2004. Aspect induced differences in vegetation, soil, and microclimatic characteristics of an Appalachian watershed. Castanea, 69(2): 92-108.

Dillen, S.Y., Op de Beeck, M., Hufkens, K., Buonanduci, M. and Phillips, N.G., 2012. Seasonal patterns of foliar reflectance in relation to photosynthetic capacity and

color index in two co-occurring tree species, Quercus rubra and Betula papyrifera. Agricultural and Forest Meteorology, 160: 60-68.

Dragoni, D. and Rahman, A.F., 2012. Trends in fall phenology across the deciduous forests of the Eastern USA. Agricultural and Forest Meteorology, 157: 96-105.

Elmore, A.J., Guinn, S.M., Minsley, B.J. and Richardson, A.D., 2012. Landscape controls on the timing of spring, autumn, and growing season length in mid-Atlantic forests. Global Change Biology, 18(2): 656-674.

Elmore, A.J., Mustard, J.F., Manning, S.J. and Lobell, D.B., 2000. Quantifying vegetation change in semiarid environments: Precision and accuracy of spectral mixture analysis and the Normalized Difference Vegetation Index. Remote Sensing of Environment, 73(1): 87-102.

Essery, R. et al., 2008. Radiative transfer modeling of a coniferous canopy characterized by airborne remote sensing. Journal of Hydrometeorology, 9(2): 228-241.

Fisher, J.I., Mustard, J.F. and Vadeboncoeur, M.A., 2006. Green leaf phenology at Landsat resolution: Scaling from the field to the satellite. Remote Sensing of Environment, 100(2): 265-279.

Fitzjarrald, D.R., Acevedo, O.C. and Moore, K.E., 2001. Climatic consequences of leaf presence in the eastern United States. Journal of Climate, 14(4): 598-614.

Flint, A.L. and Childs, S.W., 1987. Calculation of solar-radiation in mountainous terrain. Agricultural and Forest Meteorology, 40(3): 233-249.

Fridley, J.D., 2009. Downscaling Climate over Complex Terrain: High Finescale (< 1000 m) Spatial Variation of Near-Ground Temperatures in a Montane Forested Landscape (Great Smoky Mountains). Journal of Applied Meteorology and Climatology, 48(5): 1033-1049.

Garcia-Haro, F.J. and Sommer, S., 2002. A fast canopy reflectance model to simulate realistic remote sensing scenarios. Remote Sensing of Environment, 81(2-3): 205-227.

Gimenez, C., Mitchell, V.J. and Lawlor, D.W., 1992. Regulation of photosynthetic rate of two sunflower hybrids under water stress. Plant Physiology, 98(2): 516-524.

Grant, R.F., 2004. Modeling topographic effects on net ecosystem productivity of boreal black spruce forests. Tree Physiology, 24(1): 1-18.

Gu, D. and Gillespie, A., 1998. Topographic normalization of landsat TM images of forest based on subpixel Sun-canopy-sensor geometry. Remote Sensing of Environment, 64(2): 166-175.

Hall, F.G., Shimabukuro, Y.E. and Huemmrich, K.F., 1995. Remote sensing of forest biophysical structure using mixture decomposition and geometric reflectance models. Ecological Applications, 5(4): 993-1013.

Hardy, J.P. et al., 2004. Solar radiation transmission through conifer canopies. Agricultural and Forest Meteorology, 126(3-4): 257-270.

Holland, P. and Steyn, D., 1975. Vegetational responses to latitudinal variations in slope angle and aspect. Journal of Biogeography: 179-183.

Hopkins, A.D., 1918. Periodical events and natural law as guides to agricultural research and practice. US Government Printing Office.

Hwang, T. et al., 2014. Divergent phenological response to hydroclimate variability in forested mountain watersheds. Global Change Biology, 20(8): 2580-2595.

Hwang, T., Song, C.H., Bolstad, P.V. and Band, L.E., 2011. Downscaling real-time vegetation dynamics by fusing multi-temporal MODIS and Landsat NDVI in topographically complex terrain. Remote Sensing of Environment, 115(10): 2499-2512.

Jackson, M.T., 1966. Effects of microclimate of spring flowering phenology. Ecology, 47(3): 407-&.

Jeong, S.J., Ho, C.H., Gim, H.J. and Brown, M.E., 2011. Phenology shifts at start vs. end of growing season in temperate vegetation over the Northern Hemisphere for the period 1982-2008. Global Change Biology, 17(7): 2385-2399.

Keeling, C.D., Chin, J.F.S. and Whorf, T.P., 1996. Increased activity of northern vegetation inferred from atmospheric CO_2 measurements. Nature, 382(6587): 146-149.

Keenan, T.F. et al., 2014. Tracking forest phenology and seasonal physiology using digital repeat photography: a critical assessment. Ecological Applications, 24(6): 1478-1489.

Knapp, A.K. and Carter, G.A., 1998. Variability in leaf optical properties among 26 species from a broad range of habitats. American Journal of Botany, 85(7): 940-946.

Knyazikhin, Y. et al., 2013. Hyperspectral remote sensing of foliar nitrogen content. Proceedings of the National Academy of Sciences of the United States of America, 110(3): E185-E192.

Li, X.W. and Strahler, A.H., 1992. Geometric optical bidirectional reflectance modeling of the discrete crown vegetation canopy, effect of crown shape and mutual shadowing. Ieee Transactions on Geoscience and Remote Sensing, 30(2): 276-292.

Masek, J.G. et al., 2006. A Landsat surface reflectance dataset for North America, 1990-2000. Ieee Geoscience and Remote Sensing Letters, 3(1): 68-72.

Melaas, E.K., Friedl, M.A. and Zhu, Z., 2013. Detecting interannual variation in deciduous broadleaf forest phenology using Landsat TM/ETM plus data. Remote Sensing of Environment, 132: 176-185.

Menzel, A. and Fabian, P., 1999. Growing season extended in Europe. Nature, 397(6721): 659-659.

Moorthy, I., Miller, J.R. and Noland, T.L., 2008. Estimating chlorophyll concentration in conifer needles with hyperspectral data: An assessment at the needle and canopy level. Remote Sensing of Environment, 112(6): 2824-2838.

Morisette, J.T. et al., 2009. Tracking the rhythm of the seasons in the face of global change: phenological research in the 21st century. Frontiers in Ecology and the Environment, 7(5): 253-260.

Moser, L. et al., 2010. Timing and duration of European larch growing season along altitudinal gradients in the Swiss Alps. Tree Physiology, 30(2): 225-233.

Nunez, M., 1980. The calculation of solar and net-radiation in mountainous terrain. Journal of Biogeography, 7(2): 173-186.

Ogunjemiyo, S., Parker, G. and Roberts, D., 2005. Reflections in bumpy terrain: Implications of canopy surface variations for the radiation balance of vegetation. Ieee Geoscience and Remote Sensing Letters, 2(1): 90-93.

Ollinger, S.V., 2011. Sources of variability in canopy reflectance and the convergent properties of plants. New Phytologist, 189(2): 375-394.

Owenby, J.R. and Ezell, D.S., 1992. Monthly station normals of temperature, precipitation, heating and cooling degree days 1961-1990 Climatogrophy of the United States No. 81. U.S. Department of Commerce, National Oceanic and Atmospheric Administration, National Climatic Data Center, Asheville, NC, pp. 18.

Panferov, O. et al., 2001. The role of canopy structure in the spectral variation of transmission and absorption of solar radiation in vegetation canopies. Ieee Transactions on Geoscience and Remote Sensing, 39(2): 241-253.

Parker, G.G. and Russ, M.E., 2004. The canopy surface and stand development: assessing forest canopy structure and complexity with near-surface altimetry. Forest Ecology and Management, 189(1-3): 307-315.

Perry, D.A., Oren, R. and Hart, S.C., 2008. Forest ecosystems. JHU Press.

Reich, P.B., Walters, M.B. and Ellsworth, D.S., 1991. Leaf age and season influence the relationships between leaf nitrogen, leaf mass perarea and photosynthesis in maple and oak trees. Plant Cell and Environment, 14(3): 251-259.

Richardson, A.D., Bailey, A.S., Denny, E.G., Martin, C.W. and O'Keefe, J., 2006. Phenology of a northern hardwood forest canopy. Global Change Biology, 12(7): 1174-1188.

Sabol, D.E., Gillespie, A.R., Adams, J.B., Smith, M.O. and Tucker, C.J., 2002. Structural stage in Pacific Northwest forests estimated using simple mixing models of multispectral images. Remote Sensing of Environment, 80(1): 1-16.

Saxe, H., Cannell, M.G.R., Johnsen, B., Ryan, M.G. and Vourlitis, G., 2001. Tree and forest functioning in response to global warming. New Phytologist, 149(3): 369-399.

Seibt, U., Rajabi, A., Griffiths, H. and Berry, J.A., 2008. Carbon isotopes and water use efficiency: sense and sensitivity. Oecologia, 155(3): 441-454.

Shao, H.B., Chu, L.Y., Jaleel, C.A. and Zhao, C.X., 2008. Water-deficit stress-induced anatomical changes in higher plants. Comptes Rendus Biologies, 331(3): 215-225.

Slaton, M.R., Hunt, E.R. and Smith, W.K., 2001. Estimating near-infrared leaf reflectance from leaf structural characteristics. American Journal of Botany, 88(2): 278-284.

Smith, M.O., Ustin, S.L., Adams, J.B. and Gillespie, A.R., 1990. Vegetation in deserts .1. A regional measure of abundance from multispectral images. Remote Sensing of Environment, 31(1): 1-26.

Sullivan, F.B. et al., 2013. Foliar nitrogen in relation to plant traits and reflectance properties of New Hampshire forests. Canadian Journal of Forest Research-Revue Canadienne De Recherche Forestiere, 43(1): 18-27.

Tateno, R., Aikawa, T. and Takeda, H., 2005. Leaf-fall phenology along a topography-mediated environmental gradient in a cool-temperate deciduous broad-leaved forest in Japan. Journal of Forest Research, 10(4): 269-274.

Trimble, G.R. and Weitzman, S., 1956. Site index studies of upland oaks in the northern Appalachians. Forest Sci, 2((3)): 162-173.

Tucker, C.J., 1979. Red and photographic infrared linear combinations for monitoring vegetation. Remote Sensing of Environment, 8(2): 127-150.

Vitasse, Y. et al., 2009. Leaf phenology sensitivity to temperature in European trees: Do within-species populations exhibit similar responses? Agricultural and Forest Meteorology, 149(5): 735-744.

Wilson, K.B., Baldocchi, D.D. and Hanson, P.J., 2000. Spatial and seasonal variability of photosynthetic parameters and their relationship to leaf nitrogen in a deciduous forest. Tree Physiology, 20(9): 565-578.

Wilson, K.B., Baldocchi, D.D. and Hanson, P.J., 2001. Leaf age affects the seasonal pattern of photosynthetic capacity and net ecosystem exchange of carbon in a deciduous forest. Plant Cell and Environment, 24(6): 571-583.

Xu, L.K. and Baldocchi, D.D., 2003. Seasonal trends in photosynthetic parameters and stomatal conductance of blue oak (Quercus douglasii) under prolonged summer drought and high temperature. Tree Physiology, 23(13): 865-877.

Yang, X., Tang, J.W. and Mustard, J.F., 2014. Beyond leaf color: Comparing camera-based phenological metrics with leaf biochemical, biophysical, and spectral properties throughout the growing season of a temperate deciduous forest. Journal of Geophysical Research-Biogeosciences, 119(3): 181-191.

Zhang, X.Y., Friedl, M.A., Schaaf, C.B. and Strahler, A.H., 2004a. Climate controls on vegetation phenological patterns in northern mid- and high latitudes inferred from MODIS data. Global Change Biology, 10(7): 1133-1145.

Zhang, X.Y., Friedl, M.A., Schaaf, C.B., Strahler, A.H. and Schneider, A., 2004b. The footprint of urban climates on vegetation phenology. Geophysical Research Letters, 31(12).

Zhou, L.M. et al., 2001. Variations in northern vegetation activity inferred from satellite data of vegetation index during 1981 to 1999. Journal of Geophysical Research-Atmospheres, 106(D17): 20069-20083.